



Optimal Design of Riserless Test String for Deepwater Gas Hydrate

Shu-Zhan Li¹(✉), Jin Yang¹, Guo-Jing Zhu¹, Yi Huang², Jia-Kang Wang¹,
and Hong-Yu Wan¹

¹ College of Safety and Ocean Engineering, China University of Petroleum, Beijing,
Beijing 1002249, China

lishuzhan_cupb@foxmail.com

² Zhanjiang Branch of CNOOC (China) Co., Ltd., Zhanjiang 524000, China

Abstract. The South China Sea contains abundant gas hydrate resources buried in shallow layers due to geological reasons, and these resources have been difficult to utilize for a long time. In order to effectively develop subsea gas hydrate, riserless test strings are used to test the production of exploratory wells, which provides a basis for large-scale development of gas hydrate in the future. A new test stub is developed and installed at the contact position between the test string and the subsea wellhead. The interaction model of the test stub and the subsea wellhead is established, and the force characteristics of the subsea wellhead are calculated. Based on the test string structure, a riser-free test finite element model is established considering the sea wind, waves, currents and seabed soil characteristics, and the stress and deformation of test strings of different sizes under different offsets are calculated. The stress of 3.5 in, 4 in, 4.5 in and 5 in drill pipes is calculated, and it is shown that with the increase of drill pipe diameter, the extreme value of stress decreases and the extreme value of bending moment increases, but the overall variation range is not large. For the drill pipe of the same diameter, with the change of the offset of the upper platform, both the stress and the bending moment extreme value of the drill pipe increase in different magnitudes, the stress extreme value increases greatly, and the bending moment extreme value increases less. With reference to the strength of drill pipes of different sizes, a safety factor of 1.5 is used to check the test string, and it shows that drill pipes of all sizes meet

Copyright 2023, IFEDC Organizing Committee.

This paper was prepared for presentation at the 2023 International Field Exploration and Development Conference in Wuhan, China, 20–22 September 2023.

This paper was selected for presentation by the IFEDC Committee following review of information contained in an abstract submitted by the author(s). Contents of the paper, as presented, have not been reviewed by the IFEDC Technical Team and are subject to correction by the author(s). The material does not necessarily reflect any position of the IFEDC Technical Committee its members. Papers presented at the Conference are subject to publication review by Professional Team of IFEDC Technical Committee. Electronic reproduction, distribution, or storage of any part of this paper for commercial purposes without the written consent of IFEDC Organizing Committee is prohibited. Permission to reproduce in print is restricted to an abstract of not more than 300 words; illustrations may not be copied. The abstract must contain conspicuous acknowledgment of IFEDC. Contact email: paper@ifedc.org.

the conditions of use. The force of the subsea wellhead is calculated when 6-5/8 in and 5-7/8 in weighted drill pipes are used at the wellhead, and it is shown that when the platform offset is 3°, the subsea wellhead stress exceeds the allowable value and cannot be. To meet the conditions of use, it is necessary to appropriately reduce the platform offset.

The mechanical calculation of the test string without riser and the mechanical analysis of the underwater wellhead provide a basis for the design of the pipe string, which can effectively guarantee the gas hydrate test operation and lay a foundation for the large-scale development of gas hydrate in the South China Sea.

Keywords: Gas hydrate · Riserless test · String design · Subsea wellhead

1 Introduction

Global gas hydrate resources are abundant, and according to incomplete statistics, gas hydrate reserves are more than twice the amount of conventional oil and gas resources in the world, which is regarded as a strategic replacement energy source for oil and gas in the future by countries around the world [1]. Natural gas hydrate is mainly distributed in deep water subsea shallow layer and land permafrost area, among which marine gas hydrate resources are more abundant, accounting for more than 90% [2]. Geological survey results show that the Pearl River Estuary basin in the northern part of the South China Sea in China is rich in natural gas hydrate deposits [3, 4]. Moreover, gas hydrates are mainly distributed in shallow strata between tens of meters and 300 m below the mud surface of the seafloor and are found in fine-grained sediments such as muddy sands, which are characterized by shallow burial depth and poor cementation [5]. At present, there are few engineering practices for gas hydrate exploitation in marine areas, and there are many technical problems and challenges.

Reservoir testing is generally performed for gas hydrate indication and reservoir evaluation prior to long term test mining or commercial exploitation to lay the foundation for long term test mining or large scale development. The use of riserless drill string testing is a better option to save cost and simplify operation. In the process of riserless drill string testing, the test string is in constant motion under the harsh marine environment, especially at the submerged wellhead, where the stress is concentrated and constantly changing due to the contact with the wellhead, and there are large risks. For this reason, a reinforced test stub was developed and added to the test string to bring it in contact with the subsea wellhead and reduce the operational risk. During gas hydrate testing in deep-sea regions, the riserless testing string is subjected to sea wind, wave and current forces, in addition to self-weight, seawater buoyancy and internal and external fluid pressure [6]. Under the combined action of multiple loads, the static performance of the test drill string is relatively complex. The static performance is directly related to whether the structural strength and stiffness meet the requirements. Especially for the small-diameter and thin-walled structure of the test drill pipe, its static performance needs to be paid more attention. In particular, whether the developed test stubs can meet the requirements of deepwater gas hydrate testing without water trap, and whether further optimization design is needed, all need to be studied in depth.

Researchers have conducted relevant studies on the mechanical properties of deep-sea drilling tubular columns at an early stage, mainly including mechanical modeling and analytical method studies. Gosse and Barksdale [7] established a static analytical mechanical model of a deepwater drill riser and used the finite difference method to solve the differential equations for the static performance of the riser to obtain the lateral bending characteristics of the riser. Athisakul et al. [9] analyzed the static performance of a two-dimensional model of a riser with large strain characteristics in the ocean. Dawei Gong [10] established a mathematical model for the static analysis of the riser considering the rig offset and current forces, and qualitatively analyzed the force characteristics of the riser. Shi Xiaobing et al. [11, 12] used the finite unit method to calculate and analyze the deformation and load distribution law of the drilling riser, and analyzed the influence of various loads on the strength of the riser. Chang Yuanjiang et al. [13] calculated and analyzed the quasi-static performance of nonlinear deepwater drill risers based on ABAQUS software and program secondary development. Lin Xiujuan et al. [14] used the finite difference method to analyze the static mechanical properties of the drill string during the lowering of the deepwater oil recovery tree, and the effects of the drill string parameters, the marine environmental load, the drift of the drilling vessel, the operating water depth and the gravity of the oil recovery tree on the static properties of the drill string were considered in the analysis. Zhou Shouwei et al. [15] studied the static deformation characteristics of the deepwater drilling risers under the action of shear flow based on theoretical analysis and experimental tests, and put forward the “one-third effect” for the first time. The effects of the offset of the drilling vessel, water depth, weight of the bottom drilling tool assembly, current velocity, surface wave height and period on the static performance of the risers were analyzed. Li and Collins [17] reported that to eliminate buckling-induced failures, a finite element method-based analysis predicts bending moments in riserless drill strings, determining critical buckling conditions. A case study confirms the method’s accuracy in predicting failure locations, applicable to other bottom hole assemblies (BHA). Gao and Zhang [18] gave the transverse and longitudinal bending deformations and the longitudinal vibration of the drilling tubular string for the deepwater drilling operation without riser. They found that it is dangerous for the tubular string in the deepwater drilling operation without riser to work under the conditions of high or low axial tension force, deep water, severe vessel offset or heave and high speed current. Chen et al. [19] performed a torque mechanical experiment on drill string in riserless drilling. They found that the friction generated in the tangential direction when the drill string is rotating in water produces additional torque in the drill string.

Most of these studies have focused on the analysis of diaphragm morphology, and even when studies have been conducted for deepwater diaphragm-free drilling, most of them have focused on the forces on the drill string during the drilling phase, and few of them have addressed the forces on the drill string during the testing phase. In summary, the force analysis of the drill string under the load of the marine environment during the riserless testing of deepwater gas hydrate is still rare. Therefore, it is necessary to conduct relevant studies to analyze the mechanical properties of drill string in water and casing during deepwater riserless testing to provide guidance for deepwater gas hydrate testing.

2 Modeling

During deepwater gas hydrate testing, because of its short duration, a combination of drill pipe and other test tools is generally used for release spray testing. A surface test tree is installed at the top of the test tubing column with an attached liquid control line to deliver methanol and pass through the moon pool and into the seawater. The weighted drill string is started near the wellhead, with a fulcrum installed in the wellbore and a test tool such as an anti-sand tubing string attached to the lower part. The riserless test string is often subjected to environmental loads such as sea wind, waves and currents in the marine environment as well as the load effect on it from the platform deflection that occurs, and the test string system is mechanically analyzed, see Fig. 1.

To facilitate the investigation of the response characteristics of the riserless testing system, we make the following assumptions:

1. The hydraulic pipeline possesses a slender profile, thus exerting minimal influence on the stiffness of the test string. Consequently, this model postulates the test string's characteristics as those of a homogeneous, isotropic, linearly elastic circular pipe. The characteristics of the drill string joints are assumed to be identical to those of the drill string itself.
2. The top of the test column is connected to the drilling platform, thereby constituting a displacement boundary.
3. The deformation of the test string, subjected to both its self-weight and external loading, remains limited in magnitude.
4. Under the most adverse conditions, it is assumed that the motion of ocean waves, currents, and the test column occurs within a common plane.

From the basic assumptions, upon selecting a differential segment along the test string for analysis (Fig. 2):

$$(M + dM) - M + P(x)dy + W(x)dxdy - Qdx = 0 \quad (1)$$

That is

$$\frac{dM}{dx} + P(x)\frac{dy}{dx} + W(x)dy - Q = 0 \quad (2)$$

Based on the equilibrium relationship in the horizontal direction, it can be derived that:

$$(Q + dQ) - Q + F(x, y)dx = 0 \quad (3)$$

That is

$$\frac{dQ}{dx} = -F(x, y) \quad (4)$$

By substituting Eq. (4) and $M = -EI\frac{d^4y}{dx^4}$ into Eq. (2) and differentiating with respect to x , the fourth-order differential equation governing the mechanical analysis of the test string can be obtained:

$$EI(x)\frac{d^4y}{dx^4} + P(x)\frac{d^2y}{dx^2} + W(x)\frac{d^2y}{dx^2} = F(x, t) \quad (5)$$

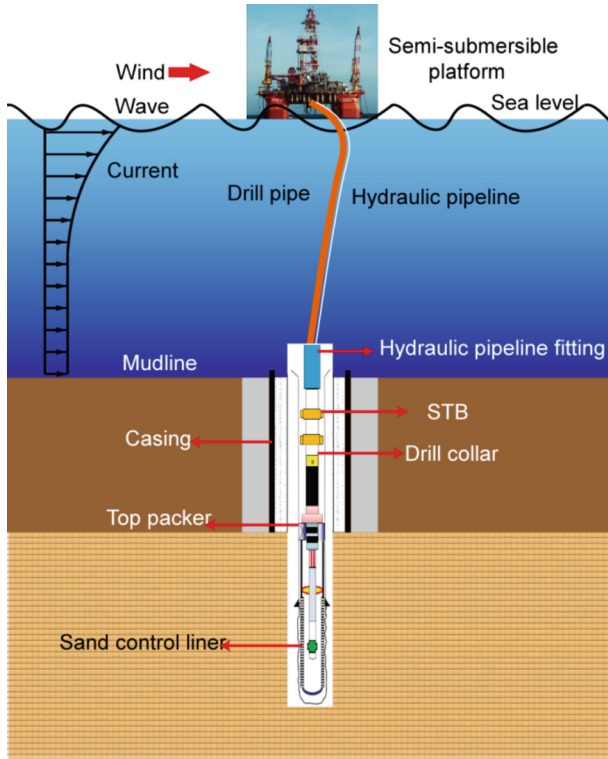


Fig. 1. Physical model diagram of drill string in deep-water riserless drilling.

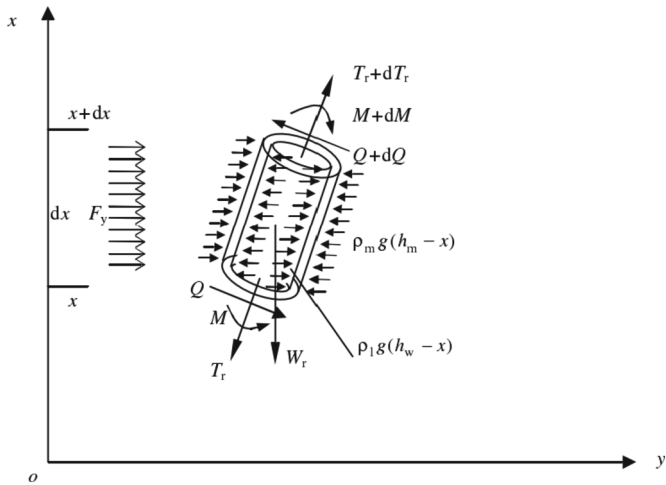


Fig. 2. Differential element of testing string

where, $EI(x)$ is the flexural stiffness of the test string along the direction; $P(x)$ is the tensile force of the test string along the x direction; $W(x)$ is the weight distribution of the test string along the x direction; $F(x, t)$ is the environmental additional load, including the load generated by wind, waves, sea currents, etc.

3 Application Examples and Mechanical Analysis of the Riserless Test String Above the Mud Line

3.1 Environmental Loads

Well X in the Lingshui block of the South China Sea was drilled at a water depth of 1,510 m. Gas hydrate was buried under the mudline in the depth range of 160 m–420 m. The test operation was conducted using a riserless drill pipe. The well was drilled and tested using a semi-submersible platform. The values of sea wind, waves and currents were taken from Table 1.

Table 1. Environmental parameters of ocean current force

Working conditions	Wave height(m)	Wave period(s)	Surface/middle/bottom current speed (m/s)	Wind speed(m/s)
Test conditions	4.8	10.5	0.99/0.45/0.30	19.1

3.2 Test Drill String Model and Simplification

The wellhead and first spud casing were 9-5/8" casing, and the depth of the first spud stage was 160 m. The end of the wellbore was an 8-1/2" bare bore section with a length of 260 m. The model was built starting from the bottom of the test tree (see Fig. 1), and the lower part was 6-5/8" drill pipe with a variable buckle connection, for a total of 1538 m. The middle wellhead contact was 10 m of a 7" OD fluid control line protection joint, and the lower part was 5-7/8" drill pipe and the gas hydrate test module. The lower part is 6-5/8" drill pipe with variable buckle connection for a total of 1538 m. 10 m of 7" OD liquid control line protection joint is in the middle wellhead contact area, and the lower part is 5-7/8" drill pipe and gas hydrate test module. Considering the location of the packer, the packer is considered as the fixed end, so the length of 5-7/8" drill pipe is 106 m. The total length of the test column is simplified to 6-5/8" drill pipe + 7" liquid control line protection joint + 5-7/8" drill pipe. The total length is 1654 m.

Modeling was performed with ANSYS finite element software, using pipe cells (see Fig. 3).

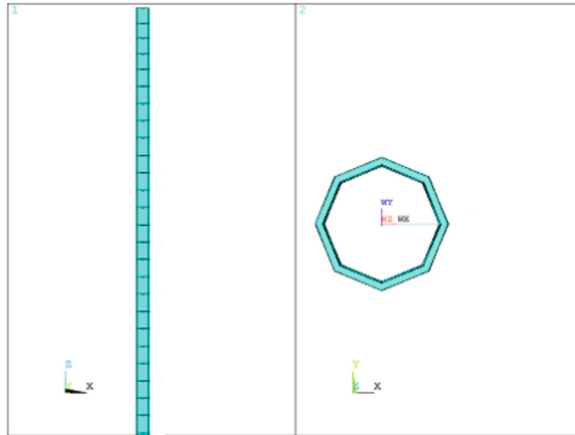


Fig. 3. Test string finite model

3.3 Boundary Conditions and Load Calculations

Gravity and Lifting Load Calculation

The weight of the drill pipe is lifted entirely from the drilling platform. The floating weight of the drill pipe is calculated in 2 parts, above the water surface and below the water surface. The full weight is 33 m above the water surface, and the float weight is 1651 m below the water surface to the bottom of the packer in seawater. The buoyancy factor is 0.87. The line weight is referred to Table 2.

The X well location is expected to use inserted test string for oil and gas testing operations, with drill pipe options ranging from 6-5/8" S-135 high-strength drill pipe to 3-1/2" drill pipe, with the following drill pipe specific parameters:

Table 2. Drill pipes parameters

Type	ID/in	OD/in	Wall thickness/in	Yield strength/Mpa	Tensile strength/Mpa	Bending stiffness/MN.m	Wire weight/ppf
3-1/2" drill pipe	3.5	2.764	0.368	1034	1000	0.393	16.1
4" drill pipe	4	3.24	0.38	1034	1000	0.626	18.24
4" heavy weight drill pipe	4	2.563	0.718	1034	826.8	0.913	27.21

(continued)

Table 2. (continued)

Type	ID/in	OD/in	Wall thickness/in	Yield strength/Mpa	Tensile strength/Mpa	Bending stiffness/MN.m	Wire weight/ppf
4-1/2" tubing	4.5	3.38	0.56	655	655	1.2	23.70
5" drill pipe	5	4.276	0.362	1034	930.1	1.25	25.12
5" heavy weight drill pipe	5	3	1	1034	965	2.33	45.77
5-7/8" drill pipe	5.875	4.971	0.452	1034	1000	2.49	30.19
5-7/8" heavy weight drill pipe	5.875	4.25	0.812	1034	1000	3.71	48.96
6-5/8" drill pipe	6.625	5.185	0.72	1034	1000	5.16	53.32

The calculated floating weight of 6-5/8" drill pipe: $G' = 1.07e6N$.

The calculated floating weight of 5-7/8" drill pipe is $G' = 6.34e5N$.

The uplift load is taken as the floating weight of the drill pipe above the packer, i.e., the load at node 1 of the model is G' .

The environmental loads are taken with reference to the environmental parameters in Table 1. Wind loads are applied between node 1 and 29 m, wave loads are applied at the sea level, and current loads are applied at the sea level - mudline.

Displacement Constraints

The top of the test string model was angled at 1°, 2°, and 3° from the bottom, and a circular casing was created at the bottom, which was set up as a universal contact with the test string to limit lateral displacement below the mudline of the test string. The bottom of the test string was set as a fixed constraint.

3.4 Finite Element Solution and Calibration

From Fig. 4, it can be seen that the displacement of 6-5/8"+7"+5-7/8" drill pipe combination at the wellhead position changes from large to small, and changes faster, and the deformation is larger here, and the phenomenon of stress concentration occurs. After calculation, from the magnitude of stress and bending moment shown in Fig. 5 and Fig. 6, it can be seen that the stress of the drill pipe near the wellhead position is the

largest, and the bending moment is also the largest. The top of the drill pipe is at an angle of 1° , 2° and 3° to the bottom respectively, and the calculated stresses are shown in Table 3. The safety factor for the mechanical properties of the test string is taken to be 1.5. Compared with the flexural yield stress and bending moment of S135 drill pipe, there is a large margin to meet the use conditions.

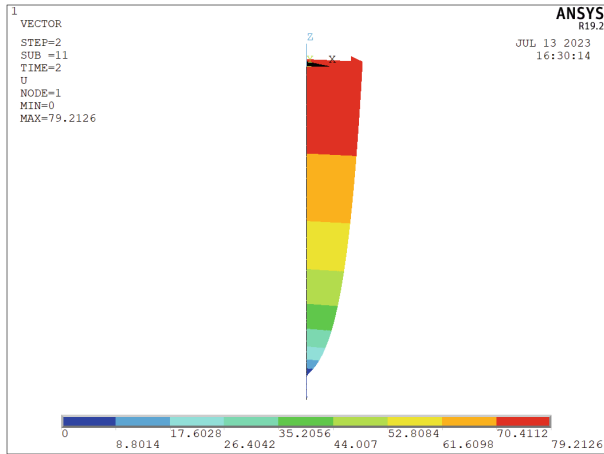


Fig. 4. Displacement cloud for 3° offset

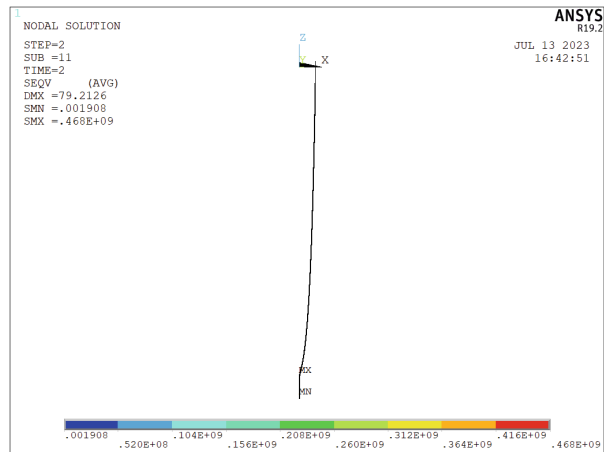


Fig. 5. Stress cloud for 3° offset

3.5 Force Analysis and Calibration of Drill Pipe of Different Specifications

The portion of the test string near and below the subsea wellhead is a combination of a 7" hydraulically controlled line protection fitting + 5-7/8" heavy weight drill pipe,

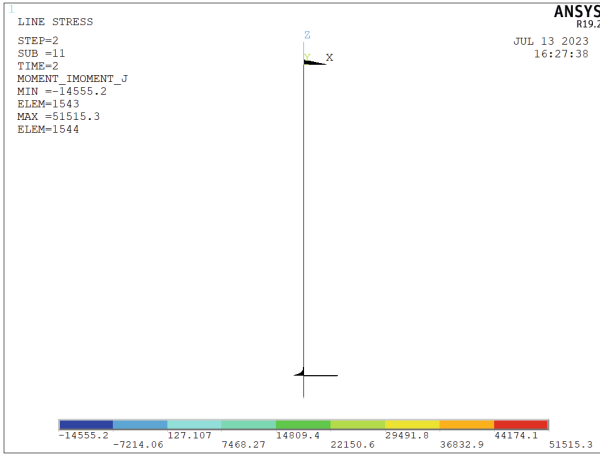


Fig. 6. Bending moment cloud for 3° offset

Table 3. Maximum stresses and bending moments in the test string

Angel	3°	2°	1°	Standard	Conclusion
Maximum stress (Mpa)	468	305	147	1034	satisfied
Maximum bending moment (N.m)	5.15E4	2.66E4	9.83E3	5.16E6	satisfied

but the test string between the subsea wellhead and the test tree above the water is available in a variety of sizes ranging from 3-1/2"-6-5/8" variations. A finite element model was developed using the method described above to solve for the maximum stress and maximum bending moment when the upper drill pipe is of different sizes, and a calibration was carried out. The results show that the maximum stresses throughout the test tubular column are in the vicinity of the contact position between the subsea wellhead and the test string, the same as the maximum bending moment.

From the calculation results in Table 4, it can be found that with the increase of platform offset, the stress on the test string increases rapidly. When the upper pipe is thinner, the maximum bending moment value of the test string is larger, and the maximum stress value shows an overall decreasing trend.

4 Force Analysis of the Wellbore Section

4.1 Finite Element Model

Taking the position of the first stabilizer as the starting point, 34 m above the 9-5/8" casing, 39 m above the test string, the upper part of the test string is 10 m 7" OD drill pipe, and the lower part is 29 m, a finite element model was built (see Fig. 7).

Table 4. Force and calibration of test columns of different sizes

Type of upper drill pipe	Angel	3°	2°	1°	Standard	Conclusion
3-1/2" drill pipe	Maximum stress (Mpa)	364	242	136	930.15	satisfied
	Maximum bending moment (N.m)	5.59E+04	4.82E+04	4.66E+03	1.48E+05	satisfied
4" drill pipe	Maximum stress (Mpa)	352	232	126	930.15	satisfied
	Maximum bending moment (N.m)	5.80E+04	4.89E+04	4.81E+03	1.48E+05	satisfied
4" heavy weight drill pipe	Maximum stress (Mpa)	395	258	133	930.15	satisfied
	Maximum bending moment (N.m)	5.97E+04	4.97E+04	5.39E+03	1.48E+05	satisfied
5" drill pipe	Maximum stress (Mpa)	306	206	77.5	930.15	satisfied
	Maximum bending moment (N.m)	6.22E+04	5.12E+04	5.39E+03	1.48E+05	satisfied
5" heavy weight drill pipe	Maximum stress (Mpa)	383	251	69.2	930.15	satisfied
	Maximum bending moment (N.m)	7.58E+04	5.66E+04	9.09E+03	1.48E+05	satisfied
4-1/2" tubing	Maximum stress (Mpa)	401	265	130	930.15	satisfied
	Maximum bending moment (N.m)	6.02E+04	4.95E+04	5.51E+03	1.48E+05	satisfied
5-7/8" drill pipe	Maximum stress (Mpa)	327	215	128	930.15	satisfied
	Maximum bending moment (N.m)	2.64E+04	1.32E+04	6.21E+03	1.48E+05	satisfied

(continued)

Table 4. (continued)

Type of upper drill pipe	Angel	3°	2°	1°	Standard	Conclusion
6-5/8" drill pipe	Maximum stress (Mpa)	468	305	147	930.15	satisfied
	Maximum bending moment (N.m)	5.15E+04	2.66E+04	9.83E+03	1.48E+05	satisfied

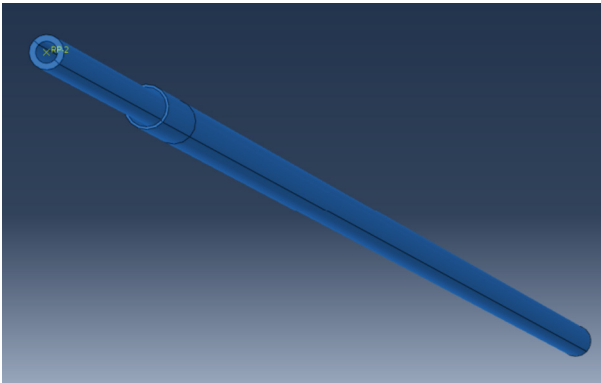


Fig. 7. Assembly model

4.2 Boundary Conditions and Load Calculations

The maximum offset is calculated as a 3° angle, the upper boundary extracts the displacement and force of the drill pipe in ANSYS, the end displacement of the 6-5/8''+7''+5-7/8'' test string combination is 0.4785 m, the end displacement of the 5-7/8''+7''+7'' test string combination is 0.334 m, the lower part is fixed, and the X and Y direction displacement is constrained below the mud line of the outer casing. The end of the "6-5/8''+7''+5-7/8'' test string is shifted by 0.4785 m, and the end of the 5-7/8''+7'' test string is shifted by 0.334 m. The lower part of the test string is fixed, and the casing is constrained to be dislocated below the mud surface of the outer side of the casing in both the X- and Y-directions.

4.3 Results and Calibration

Taking the offset of 3% of the water depth as an example, as shown in Figs. 8, 9, 10, 11 and Fig. 12, the maximum stress of 6-5/8''+7''+5-7/8'' combination test string is 251.3 MPa at the position in contact with the casing, and the maximum stress of casing is 521.6 MPa at the wellhead. The yield strength of P110 grade casing is 862 MPa, and the safety coefficient is 1.65, which meets the requirements. The deformation difference of the whole casing end face is 1.4e-3 m, i.e. 1.4 mm, which is 0.57% compared with

the interface diameter of 9-5/8" casing. The amount of deformation is not large enough for the test string to be removed (Table 5).

Table 5. Casing stresses and deformations of 6-5/8"+7"+5-7/8" combination test string

Offset	Casing /in	Edge deflection/mm	Stress/MPa	Yield strength/MPa	Safety factor	conclusion
3%	9-5/8	1.4	521.6	862	1.65	satisfied
3°	9-5/8	2.57	975.7	862	-	unsatisfied

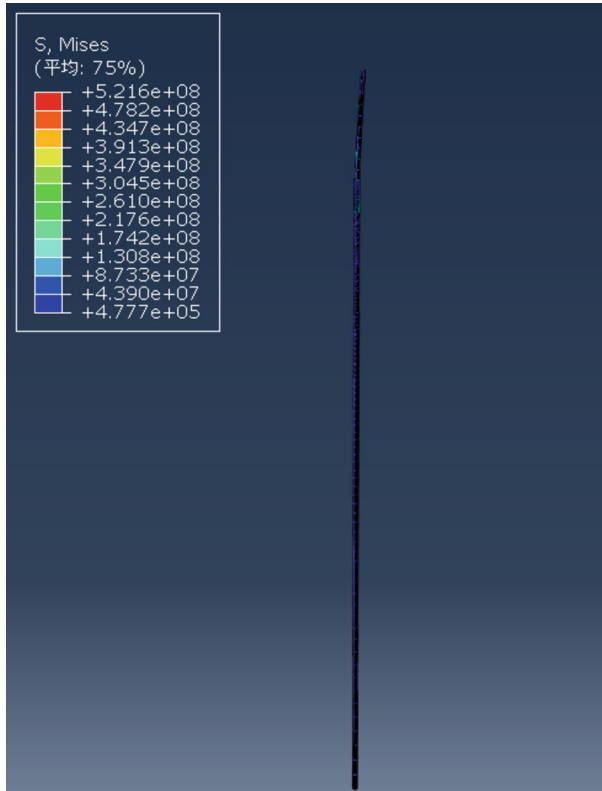


Fig. 8. Overall stress distribution

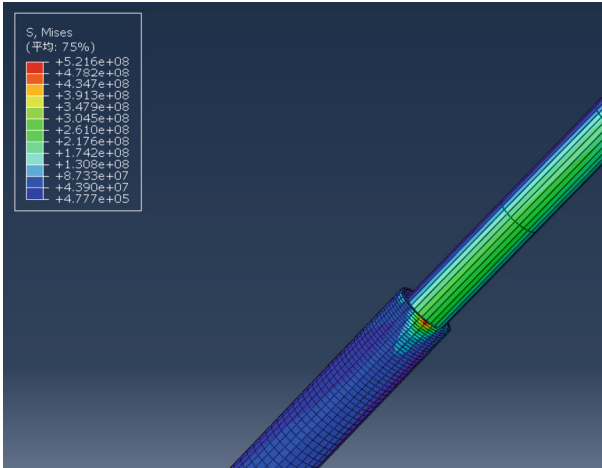


Fig. 9. Maximum stress display

Taking the offset of 3% of the water depth as an example, the maximum stress of 5-7/8''+7''+5-7/8'' combination test string is 155.3 MPa at the position in contact with the casing, and the maximum stress of casing is 313.1 MPa at the wellhead. The yield strength of P110 grade casing is 862 MPa, and the safety coefficient is 2.75, which meets the requirements. The deformation difference of the whole casing end face is 8.4e-4 m, i.e. 0.84 mm, which is 0.34% compared with the interface diameter of 9-5/8'' casing. The amount of deformation is not large enough for the test string to be removed (Table 6).

Table 6. Casing stresses and deformations of 5-7/8''+7''+5-7/8'' combination test string

Offset	Casing /in	Edge deflection/mm	Stress/MPa	Yield strength/MPa	Safety factor	conclusion
3%	9-5/8	0.84	155.3	862	2.75	satisfied
3°	9-5/8	1.55	579.7	862	1.49	unsatisfied

After calculation and analysis, the composition of 4 in heavy weight drill pipe +7 in hydraulically controlled line protection fitting+ 5-7/8 in heavy weight drill pipe was finally adopted for the site construction.

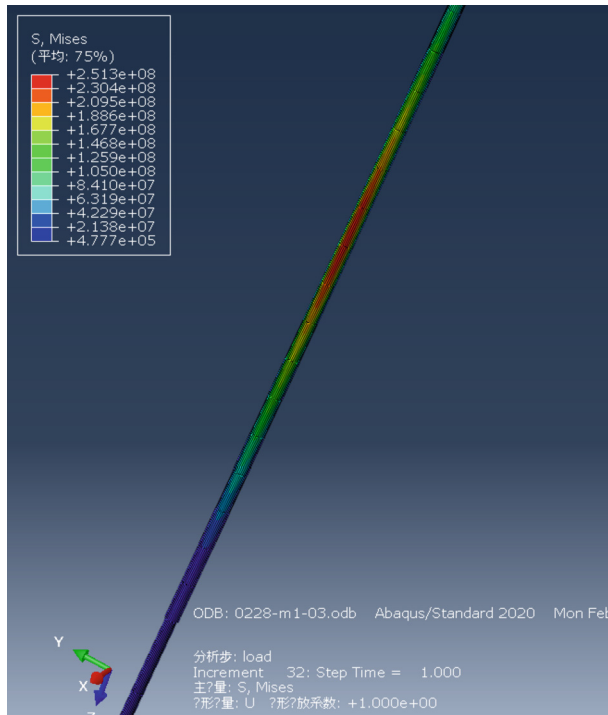


Fig. 10. Stress distribution in drill pipe

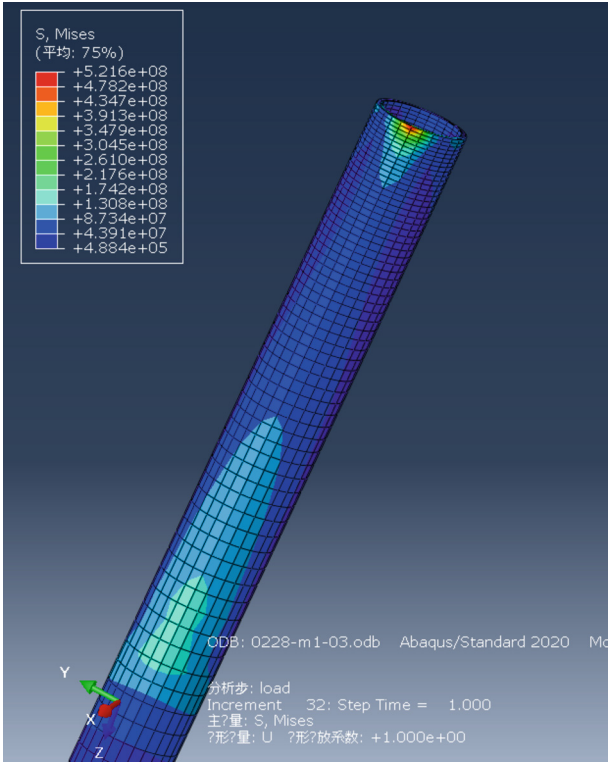


Fig. 11. Casing stress distribution

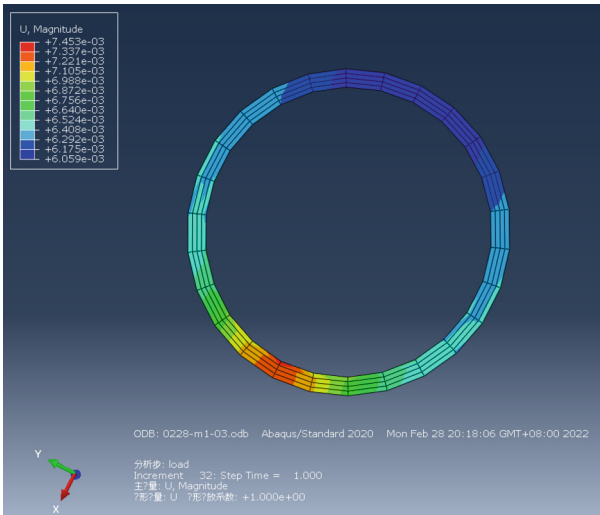


Fig. 12. Deformation of casing end face

5 Conclusion

1. According to the environmental load of the X well location, a finite element model of the test string was established, and the mechanical characterization was carried out using finite element software, and the results are instructive for optimizing the design of the test string.
2. With the increase of platform offset, the force on the test string increases rapidly. The finer the upper drill pipe is, the larger the maximum bending moment value of the test string is, and the maximum stress value shows an overall decreasing trend.
3. The model below the mud line of the test string is established to more accurately analyze the interaction between the test string and the casing. Because of the thin wall thickness of the casing, the force is greatest at the wellhead, and the cross-sectional deformation of the casing is also greatest at the wellhead, which is the weakest position of the casing.
4. The casing force analysis of 5-7/8"+7"+5-7/8" drill pipe combination shows that the casing force does not meet the use conditions when the platform offset is 3 degrees from the subsea wellhead. When the platform offset is 3% of the water depth, the casing force meets the use conditions. The casing force of test string with upper size less than 5-7/8" meets the requirement.

Acknowledgments. The project is supported by National Natural Science Foundation of China (No. U22B20126), National Key Research and Development Program (No. 2022YFC2806100) and National Ministry of Industry and Information Technology Innovation Special Project (No. 2020-HGCBGXZG-ZX-GCFW-1780).

References

1. Li, W.L., Gao, D.L., Yang, J.: Challenges and prospect of the drilling and completion technologies used for the natural gas hydrate reservoirs in sea areas. *Oil Drilling Prod. Technol.* **41**(6), 681–689 (2019)
2. Merey, S.: Drilling of gas hydrate reservoirs. *J. Nat. Gas Sci. Eng.* **35**, 1167–1179 (2016)
3. Zhong, G.J., Zhang, R.W., Yi, H., et al.: The characteristics of shallow gas reservoir developed in the northern continental slope of South China Sea. *J. Trop. Oceanogr.* **37**(3), 80–85 (2018)
4. Qi, Z.H.: Exploration of regional geologic differences in the northern part of the South China Sea and the relationship between gas hydrate formation and reservoir formation. *China Petrol. Chem. Stand. Qual.* **37**(3), 80–85 (2018)
5. Li, L.L., Yang, J., Lu, B.P., et al.: Research on stratum settlement and wellhead stability in deep water during hydrate production testing. *Petrol. Drilling Tech.* **48**(05), 61–68 (2020)
6. Gao, G.H.: Study on Static Performance and Dynamic Response of the Deep-Sea Axial-Tensioned Riser. Qingdao, China University of Petroleum (2020)
7. Gosse, C.G., Barksdale, G.L.: The marine riser-a procedure for analysis. In: *Offshore Technology Conference*, Houston, Texas, USA, OTC-1080 (1969)
8. Burke, B.G.: An analysis of marine risers for deep water. *J. Petrol. Technol.* **26**(4), 455–465 (1974)
9. Athisakul, C., Huang, T., Chucheepsakul, S.: Large strain static analysis of marine risers via a variational approach. In: *The Twelfth International Offshore and Polar Engineering Conference*, Kitakyushu, Japan, ISOPE-I-02-158 (2002)

10. Gong, D.W.: The analysis of the capacities of the marine riser. In: Ocean Engineering Conference, pp. 334–340 (2003)
11. Shi, X.B., Guo, Z.X., Nie, R.G., et al.: Study on deformation and load distribution law of marine riser for offshore deep drilling. *Nat. Gas Ind.* **24**(3), 88–90 (2004)
12. Shi, X.B., Chen, P.: Influence of 3-D loads on strength of marine riser for off-shore deep drilling. *Nat. Gas Ind.* **24**(3), 88–90 (2004)
13. Chang, Y.J., Chen, G.M., Sun, Y.Y., et al.: Quasi-static nonlinear analysis of deepwater drilling risers. *J. China Univ. Petrol. (Ed. Nat. Sci.)* **24**(3), 88–90 (2004)
14. Lin, X.J., Xiao, W.S., Wang, H.Y.: Drill string mechanical analysis of running deepwater oil tree. *J. China Univ. Petrol. (Ed. Nat. Sci.)* **35**(5), 125–129 (2011)
15. Zhou, S.W., Liu, Q.Y., Jiang, W., et al.: The discovery of “one third effect” for deep water drilling riser: based on the theoretical and experimental study of deformation characteristics of deep water drilling riser by ocean currents. *China Offshore Oil Gas* **25**(6), 1–7 (2013)
16. Wang, Y.B., Gao, D.L., Fang, J.: Static analysis of deep-water marine riser subjected to both axial and lateral forces in its installation. *J. Nat. Gas Sci. Eng.* **19**, 84–90 (2014)
17. Li, K., Collins, T.: A method for buckling analysis of a riserless drill string. In: SPE/Deepwater Drilling and Completions Conference, TX (2010)
18. Gao, D.L., Zhang, H.: Mechanical analysis of tubes in deepwater drilling operation without riser. *Tech. Rev.* **30**, 37–42 (2012)
19. Chen, W., Fu, H.Q., Lin, C.K., et al.: Experimental investigation of the torque of the drilling string for ocean scientific riserless drilling. *Chin. J. Appl. Mech.* **38**, 663–669 (2021)